Biochimica et Biophysica Acta, 1149 (1993) 267–277

BBAMEM 76017

Structure of the apolipoprotein A-IV/lipid discoidal complexes: an attenuated total reflection polarized Fourier transform infrared spectroscopy study

Laurence Lins [a], Robert Brasseur [a], Maryvonne Rosseneu [b], Berlinda Vanloo [b] and Jean-Marie Ruysschaert [a]

[a] *Laboratoire de Chimie Physique des Macromolécules aux Interfaces, Free University of Brussels, Brussels (Belgium) and* [b] *Department of Clinical Chemistry, A.Z. St. Jan, Bruges (Belgium)*

(Received 25 January 1993)

Key words: Apolipoprotein A-IV; HDL; Reconstituted HDL; Amphipathic helix; Infrared spectroscopy; FTIR

Discoidal lipid particles were prepared from a reaction mixture containing apo A-IV and dimyristoylphosphatidylcholine (DMPC) or dipalmitoylphosphatidylcholine (DPPC) in the molar ratio of 185:1 (lipid/protein). The complexes were isolated by gel filtration and characterized in terms of composition and size. Infrared attenuated total reflection spectroscopy was used to estimate the secondary structure of apolipoprotein A-IV and the orientation of its amphipathic α-helices with respect to the lipid hydrocarbon chains. In addition, infrared spectra were analyzed in terms of the conformation and organization of different regions of the lipid molecules in the particles. This approach has been applied successfully to reconstituted HDL particles prepared from a reaction mixture containing DPPC and apo A-I in the molar ratio of 150:1 (Wald, J.H., Goormaghtigh, E., De Meutter, J., Ruysschaert, J.M. and Jonas, A. (1990) J. Biol. Chem. 265, 20044–20050). Apo A-IV helicity increased for the protein bound to DMPC or DPPC but the increase was more pronounced for the apo A-IV/DMPC particles. In both complexes, the α helical amphipathic segments of the protein were parallel to the lipid acyl chains and no significant modification of the overall organization of the lipid molecules in the lipid bilayer was observed. The presence of apo A-IV seems only to affect the conformation of the lipid hydrocarbon chains in close contact with the protein in the discoidal particles.

Introduction

Apolipoprotein A-IV is a 46-kDa glycoprotein described for the first time in rats [1] and later in other species including humans [2,3]. This protein is known to associate with mesentric chylomicrons, as well as apo A-I [2]. After their entry into circulation, chylomicrons undergo changes, including rapid dissociation of apo A-I and A-IV and exchange with apo E and C [4,5]. Apo A-I reassociates mainly with high density lipoproteins (HDL) while apo A-IV is distributed between the HDL fraction and the lipoprotein free fraction (LFF) [6,7].

Although no specific function has been attributed to apo A-IV, this protein participates to the HDL metabolism because it redistributes from LFF to the HDL_3 fraction during cholesterol esterification by the LCAT (lecithin cholesterol acyltransferase) enzyme [8–10], and leaves the HDL surface when lipid transfer proteins (cholesteryl ester transfer protein, phospholipid transfer protein, etc.) act on those particles [11,12]. Apo A-IV is also related to the reverse cholesterol transport by its ability to promote cellular cholesterol efflux [13,14], to specifically bind to rat hepatocytes [15,16] and aortic endothelial cells [17,18] and to activate lecithin cholesterol acyltransferase in vitro [19,20]. Discoidal particles composed of phospholipids, cholesterol and apo A-IV have been identified in the peripheral lymph of cholesterol fed animals [21,22] and of humans [22].

The effect of lipids on the structure and orientation of human apo A-I has been intensively investigated by a variety of biophysical approaches [23–28]. Such techniques have not been applied so systematically to examine the structure–function relationship of human apo A-IV and available information are much more limited [12,29]. We describe here our attempt to determine the structure of the reconstituted apo A-IV/phospholipid discoidal complexes. Since it is generally accepted that usual algorithms (Chou-Fasman, Garnier) cannot be applied to predict the structure of

Correspondence to: L. Lins, Laboratoire de Chimie Physique des Macromolécules aux Interfaces, Free University of Brussels, Bd du Triomphe, 1050 Brussels, Belgium.

membrane proteins and because circular dichroism (CD) is subject to artefact due to protein or lipid aggregation, infrared spectroscopy has been used to provide information about the structure of lipid associated proteins. The IR approach has been applied to several membrane systems [24,30–34] and has been used here to estimate the content of secondary structure of apo A-IV in the lipid complex and the orientation of its secondary domains with respect to the phospholipid hydrocarbon chains. The IR spectra were also analyzed in terms of the conformation and organization of different domains of the lipid molecules in the discoidal complexes.

Materials and Methods

Isolation and purification of human apo A-IV

Apo A-IV was obtained from chylous ascites fluid from a single patient [35]. After chylomicra isolation at a density of 1.006 g/ml, the chylomicra were first delipidated by extraction with acetone/ethanol (1:1 (v/v)) and hexane/isopropanol (3:2 (v/v)) and finally with n-hexane. Apo A-IV was isolated by FPLC on a Mono-Q 10/10 HR anion-exchange column [35]. Purity of the fractions was checked by SDS-PAGE and isofocusing.

Preparation of the apo A-IV/phospholipid complexes

Discoidal complexes were spontaneously obtained by incubation of apo A-IV and sonicated small unilamellar vesicles of DMPC (dimyristoylphosphatidylcholine) (Sigma) in a 1:3 (w/w) ratio (1:185 molar ratio), overnight at 24°C. The cholate dialysis method [36] was used for the preparation of complexes of apo A-IV with synthetic DPPC (dipalmitoylphosphatidylcholine, Sigma). Reconstituted particles were prepared as for apo A-IV/DMPC (1:3 (w/w)), by adding apo A-IV at a concentration of 1 mg/ml to 0.5 ml of the corresponding phospholipid mixture dispersion in sodium cholate (1:1 (w/w), lipid/cholate). This mixture was incubated overnight at 42°C and extensively dialysed at 42°C against a Tris 10 mM, NaCl 0.15 M, NaN_3 1 mM, EDTA 0.01% buffer (pH 8).

Characterization of the discoidal complexes

Apo A-IV/DMPC or DPPC complexes were isolated by gel chromatography on a Superose 6HR column in a 0.01 M Tris-HCl (pH 7.6) buffer [37]. For the detection of the complexes, the absorbance was continuously monitored at 280 nm and the Trp emission of each fraction was measured on a Jasco SFP 500 spectrofluorimeter; the phospholipid content was determined by an available kit (Boehringer-Mannheim). For further evaluation of the composition and size of the complexes, the top fractions of the elution peak in the chromatographic runs were collected. The composition of these fractions was determined by quantitation of the phospholipids using a colorimetric enzymatic assay (Boehringer-Mannheim). Protein concentration was estimated by dosage of Phe residues by HPLC on a C_{18} reverse-phase column, after protein hydrolysis [37]. The size of the complexes was estimated by electron microscopy after negative staining with a 20 g/l solution of potassium phosphotungstate (pH 7.4). 7 μl of the sample were applied to Formvar carbon-coated grids and examined on a Zeiss EM 10 C transmission electron microscope operating at 60 kV. Particles' size was determined by measuring 50 discrete particles/sample. The Stokes diameters of the complexes were also estimated by nondenaturing gradient gel electrophoresis using Pharmacia PAA 4/30 gels. A Tris-boric acid (pH 8.4) buffer was used and electrophoresis was conducted under 150 V for 19 h. The gels were stained with Coomassie blue and scanned with a laser densitometer (Pharmacia). Proteins with known Stokes radii were used as standards: bovine serum albumine (71 Å Stokes diameter), lactate dehydrogenase (81 Å), catalase (104 Å), horse ferritin (122 Å) and thyroglobulin (170 Å) (Calibration kit, Pharmacia).

Infrared spectroscopy

Attenuated total reflection (ATR) infrared spectroscopy was used to determine the secondary structure of apo A-IV and the relative orientation of the helical segments and the phospholipid acyl chains with respect to the plane of the germanium crystal, as previously described for apo A-I, apo A-II, CNBr apo A-I fragments-phospholipids complexes and LDL [24,25,37,38].

Spectra were recorded on a Perkin-Elmer 1720 X spectrophotometer equipped with a liquid nitrogen-cooled MCT detector, at a resolution of 4 cm^{-1}, by averaging 128 scans. Every four scans, reference spectra of a clean germanium plate were automatically recorded and ratioed against the recently run sample spectra by an automatic sample shuttle accessory. The spectrophotometer was continuously purged with dry air. For polarization experiments, a Perkin-Elmer gold-wire polarizer was placed in front of the sample or the reference plate. The internal reflection element was a germanium ATR plate ($50 \times 20 \times 2$ mm, Harrick EJ2121) with an aperture angle of 45° yielding 25 internal reflections.

Each complex containing 0.1 mg of apo A-IV was washed against 5 mM Tris buffer (pH 7.6) in eight consecutive dilution-concentration cycles using a Centricon 30000 microconcentrator unit (Amicon) [24].

Each sample was deposited on the germanium plate and dried gently under N_2. About the preservation of the disc structure upon drying, it must be emphasized that the discoidal structure of the complex has been

extensively assessed, among other techniques, by electron microscopy of negatively-stained samples, a technique which involves a dehydration step. We are therefore confident that the transfer of the discoidal particles on the germanium crystal and the rehydration with D_2O does not change their structure in a major way. It should also be mentioned that the apo B-100 [38] secondary structure in low-density lipoproteins has been shown to be identical in solution and deposited on the germanium plate

The plate was then sealed in an universal sample holder and rehydrated by flushing the chamber of the holder with N_2 saturated with D_2O for 3 h at room temperature, in order to avoid overlapping of the absorption bands corresponding to random and α-helical structures [39].

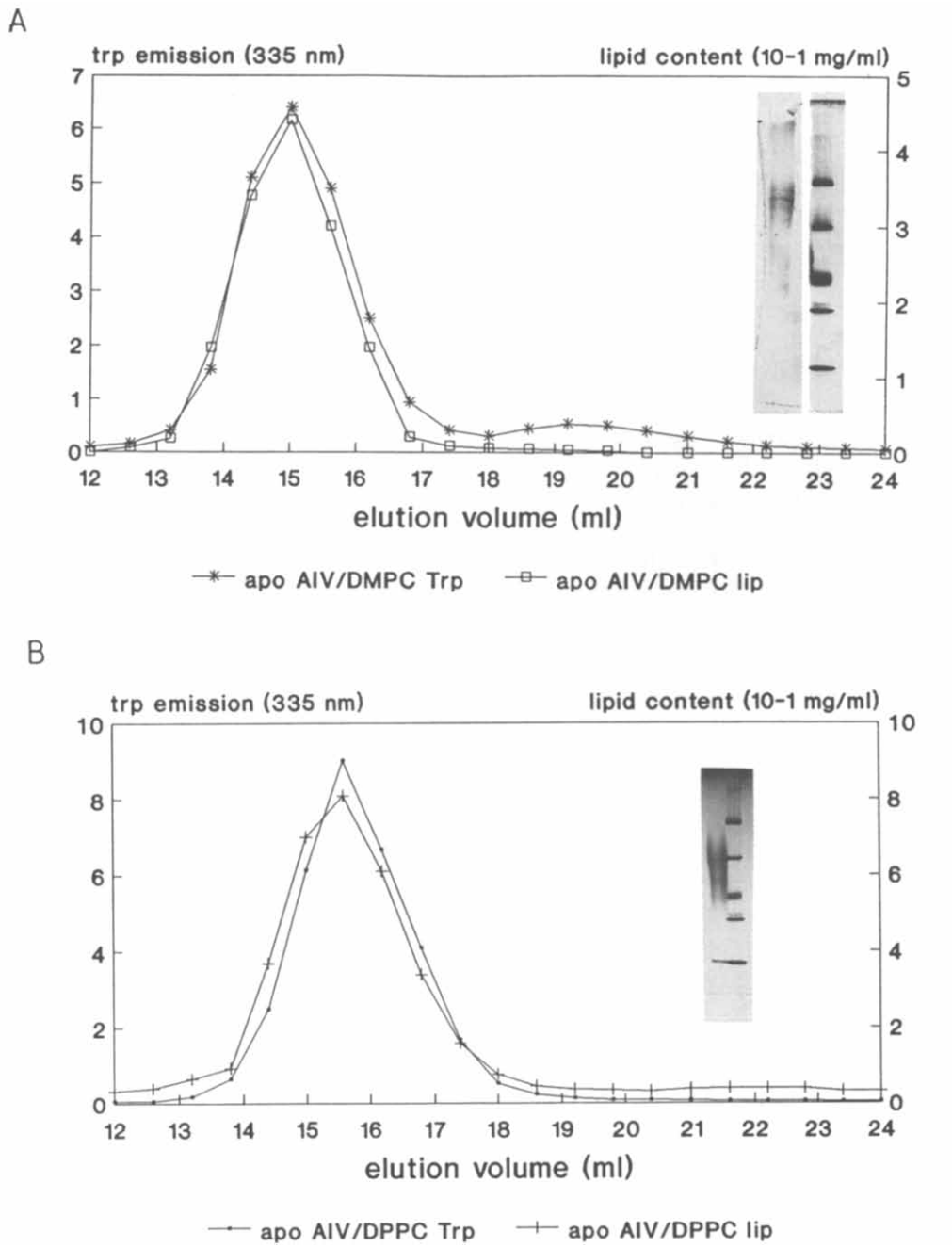

Fig. 1. Purification of the apo A-IV/DMPC (A) and apo A-IV/DPPC (B) reconstituted discs, generated at an initial phospholipid/protein ratio of 3:1 (w/w) by gel filtration on a Superose 6 HR. The concentration of the lipid (10^{-1} mg/ml, right y-axis) and the relative Trp intensity (left y-axis) are represented as a function of the elution volume. Insets Fig. 1: Gradient gel electrophoresis separation of the three top fractions (left lane) of the apo A-IV/DMPC (A) and apo A-IV/DPPC (B) reconstituted discs, carried out in a 4–30% acrylamide gradient. The Stokes diameters (Table I) were determined by comparison with known standards (right lane: standards, from top to bottom: thyroglobulin, ferritin, catalase, lactate dehydrogenase, bovine serum albumin) after scanning of the gels.

The complexes were stable at least for one week, as checked by re-isolation on the Superose column and by evaluation of the secondary structure of apo A-IV one week after the complex formation.

Secondary structure estimation and orientation of the protein and the phospholipids

Secondary structure of apo A-IV and orientation of the protein and phospholipid component were determined as described in Ref. 24. Briefly, the secondary structure is determined from self-deconvolution by Fourier transform and curve fitting of the amide-I′ region (1600–1700 cm^{-1}) of the spectrum. When orientation has to be evaluated, spectra are recorded at two orthogonal linear polarizations (90° and 0°) of the incident light. A dichroic spectrum was obtained by subtracting the spectrum recorded with polarized light at 0° from that at 90°. The angle between a normal to the Ge crystal and the dipole is calculated from the dichroic ratio R_{ATR}:

$$R_{ATR} = \frac{A(90°)}{A(0°)} \quad (1)$$

where $A(90°)$ is the absorbance of the selected dipole from a spectrum recorded with polarized light at 90° and $A(0°)$ the absorbance of the same dipole from a 0° polarized spectrum.

The bands chosen to characterize the protein and phospholipid orientation are those described in Ref. 24.

Results

Separation and characterization of the DMPC / apo A-IV and DPPC / apo A-IV complexes

The lipid/protein complexes prepared from a reaction mixture containing apo A-IV and DPPC or DMPC in a 185 : 1 lipid/protein molar ratio were fractionated on a Superose 6 HR column (Fig. 1). The presence of apo A-IV in each fraction was detected by Trp emission at 335 nm and the concentration of phospholipids was determined by an enzymatic colorimetric assay.

In the DMPC/apo A-IV complexes, a small amount a free apo A-IV eluted at 18–21 ml while for DPPC/apo A-IV complexes, no free protein nor free lipids were detected (Fig. 1).

The composition (Table I) of the complexes corresponding to the top of the elution peak in the chromatographic elution pattern (Fig. 1) was determined by phospholipid and protein assays. Electron microscopy of the DMPC and DPPC complexes revealed the typical pattern of rouleaux, characteristic of stacked discs (data not shown).

The Stokes radii determined by non denaturing gradient gel electrophoresis (GGE) (Fig. 1, inset) were 67 Å, 71 Å and 75 Å for the DMPC complexes (Fig. 1A) and 56 Å, 60 Å and 62 Å for the DPPC complexes (Fig. 1B). Electron microscopy revealed for both complexes a diameter about 20 Å larger than that determined by GGE (Table I); this discrepancy could be explained in terms of flattening of the complexes during sample preparation and electron irradiation [37,40].

Infrared experiments

Secondary structure of apo A-IV in the DMPC / apo A-IV and DPPC / apo A-IV complexes. The secondary structure of apo A-IV was estimated from the amide-I′ region of the spectra (1689–1615 cm^{-1}) after Fourier self deconvolution and curve fitting (Fig. 2). Table II summarizes the percentage of each secondary structure as compared to native apo A-IV: an increase of 10–15% helicity is observed when apo A-IV is bound to DPPC and 20–25% when DMPC is the phospholipid present in the reconstituted particles.

Orientation of the apo A-IV α-helices and the phospholipid hydrocarbon chains. Spectra were recorded with polarized light at 0 and 90° (Fig. 3). A larger absorbance at 90° for the amide-I′ vibration at 1654 cm^{-1} is observed on the DPPC/apo A-IV dichroic spectrum (Fig. 3A), resulting from the subtraction of the spectrum recorded with a 0° polarized light from that recorded at 90°. Spectra with similar pattern were recorded for the DMPC/apo A-IV complex (data not shown). This amide-I′ deviation indicates a dipole

TABLE I

Composition and size of the apo A-IV / dimyristoylphosphatidylcholine and apo A-IV / dipalmitoylphosphatidylcholine complexes

	Inubated mixture w/w ratio	Isolated complex w/w ratio	Isolated complex molar ratio	Stokes diameter [a] (Å)	EM diameter [b] (Å)
Apo A-IV/DMPC	3:1	3.8:1	258:1	134–150 (±5)	165±19
Apo A-IV/DPPC	3:1	2.9:1	182:1	112–124 (±5)	138±13

[a] Obtained from gradient gel electrophoresis gels by reference to standard proteins. The reproducibility of the diameter measurements is within ±5 Å.

[b] Measured from electron micrographs of negatively stained samples. Mean ± S.D. of the diameters are given for $n = 50$.

preferentially oriented perpendicular to the Ge plate. The dichroic ratios (Table III) of the α-helix components in the DPPC/apo A-IV and DMPC/apo A-IV complexes, calculated as described in Materials and Methods, are 1.60 and 1.65, corresponding to angles between the helix axis and the normal to the Ge crystal of 27° and 25°, respectively.

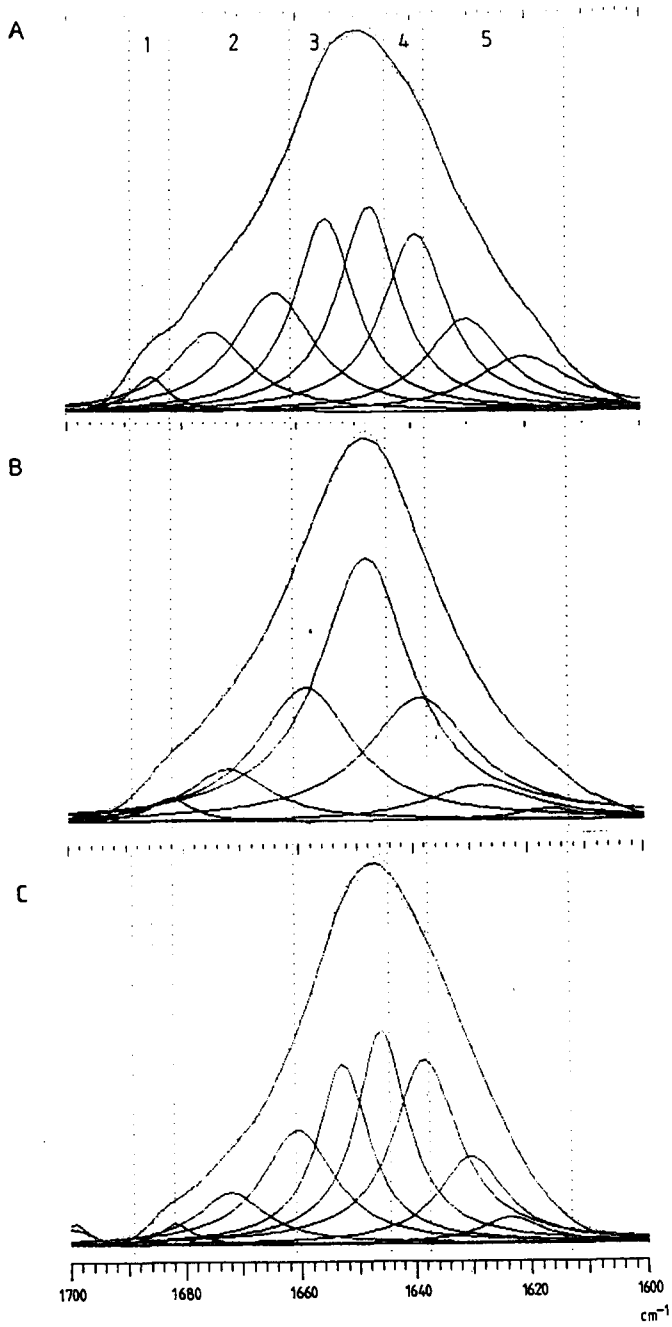

Fig. 2. Fourier self-deconvolved IR spectra of deuterated free apo A-IV (A), apo A-IV/DMPC (B) and apo A-IV/DPPC (C) recorded in the amide-I′ region. The initial output parameters for the curve fitting were determined after Fourier self-deconvolution of the spectra as described in Ref. 30. The fitting had a root mean square better than 0.015. The vertical dotted lines delimit the regions of the spectra assigned to the secondary structures: regions 1 and 5, β sheet; region 2, β turn; region 3, α helix; region 4, coil.

TABLE II

Determination of the secondary structure of apo A-IV alone or reconstituted with phospholipids after deconvolution and curve-fitting of the amide-I′ IR region (see Fig. 2)

	α-helix (%)	β-sheets (%)	Random (%)	β-turn (%)
Native apo A-IV	37±4	22±2	17±2	24±2
Apo A-IV/DMPC	58±6	16±2	15±2	11±2
Apo A-IV/DPPC	47±5	19±2	19±2	15±2

Since the transition dipole moment of the $\gamma_w(CH_2)$ peak at 1200 cm^{-1} lies along the all-*trans* acyl chains, this peak was chosen to characterize the hydrocarbon-chain orientation in the DMPC and DPPC bilayers. The strong 90° polarization of this peak (Fig. 3A) and the corresponding values of the dichroic ratios (Table III) indicate that the all-*trans* acyl chains are oriented parallel to a normal to the Ge surface.

Comparison of the orientations suggests that the α-helices of apo A-IV and the DPPC or DMPC hydrocarbon chains lie mainly parallel to each other in both reconstitutions, in agreement with the orientations obtained for heterogeneous apo A-I/DMPC reconstituted HDL [25] or for homogeneous apo A-I/DPPC reconstituted HDL [24] and confirms a structural model in which the α-helices of the apolipoproteins lie parallel to the phospholipid acyl chains on the periphery of the discoidal structure [25,41].

Modifications of the phospholipid structure and orientation induced by the presence of apo A-IV in the DMPC / apo A-IV and DPPC / apo A-IV complexes. Results are only shown for the DPPC complexes as compared to pure DPPC, but identical observations were made for the DMPC complexes (data not shown).

(1) Hydrocarbon chain conformation: The hydrocarbon chain in the α position of the DMPC or DPPC in the gel state is all trans from the ester group down to the methyl group. The resonance between the ester group and the $-CH_2$ groups of the acyl chain gives rise to the so-called $\gamma_w(CH_2)$ progression between 1200 and 1350 cm^{-1} (for DMPC: peaks at 1204, 1230, 1257, 1280, 1303 and 1327 cm^{-1}; and for DPPC: peaks at 1199, 1222, 1247, 1268, 1286, 1309, 1326 and 1344 cm^{-1}). The proportion of the α chains in the all-*trans* conformation can be evaluated from the area of one of these bands (1200 cm^{-1}) relative to the $\nu(C=O)$ band at 1737 cm^{-1} that is not sensitive to conformation. Comparison of these ratios for pure DPPC and the apo A-IV/DPPC complex, reveals a significant decrease of 25% for the complex. It could be due to the appearance of a kink somewhere between C-2 and C-16 of the chain, but a kink would reduce the number of bands in the progression. Since the same number of progression bands can be identified in the apo A-IV/DPPC spec-

tra (Fig. 3A) as in the pure DPPC spectra (Fig. 3B), this decreased area could be explained by a limited conformational change at the level of the ester group of all the phospholipids present in the complexes or at the level of the acyl chains of the lipids which are in close contact with the apo A-IV at the periphery of the disc. Indeed, 25% effect coincides with the proportion of DMPC or DPPC molecules calculated to be adjacent to apo A-IV in reconstituted particles.

(2) Orientation of the acyl chains: the dichroic ratios obtained for apo A-IV/DPPC complexes and DPPC liposomes were 4.5 and 3.2, corresponding to angles of 18° and 23°, respectively, with respect to a normal to the Ge crystal. The R_{ATR} values for pure DMPC and DMPC-containing complexes were 6.3 and 7.1, respectively, corresponding to angles of 15° and 14°. From these data, it can be concluded that the apo A-IV-lipid interaction does not modify the lipid orientation.

(3) Ester group region: the $C-\overset{\overset{O}{\|}}{C}-O-C$ segment of the fatty acyl-glycerol bond in the α-position is planar, and the corresponding ν(C–O) vibration occurs

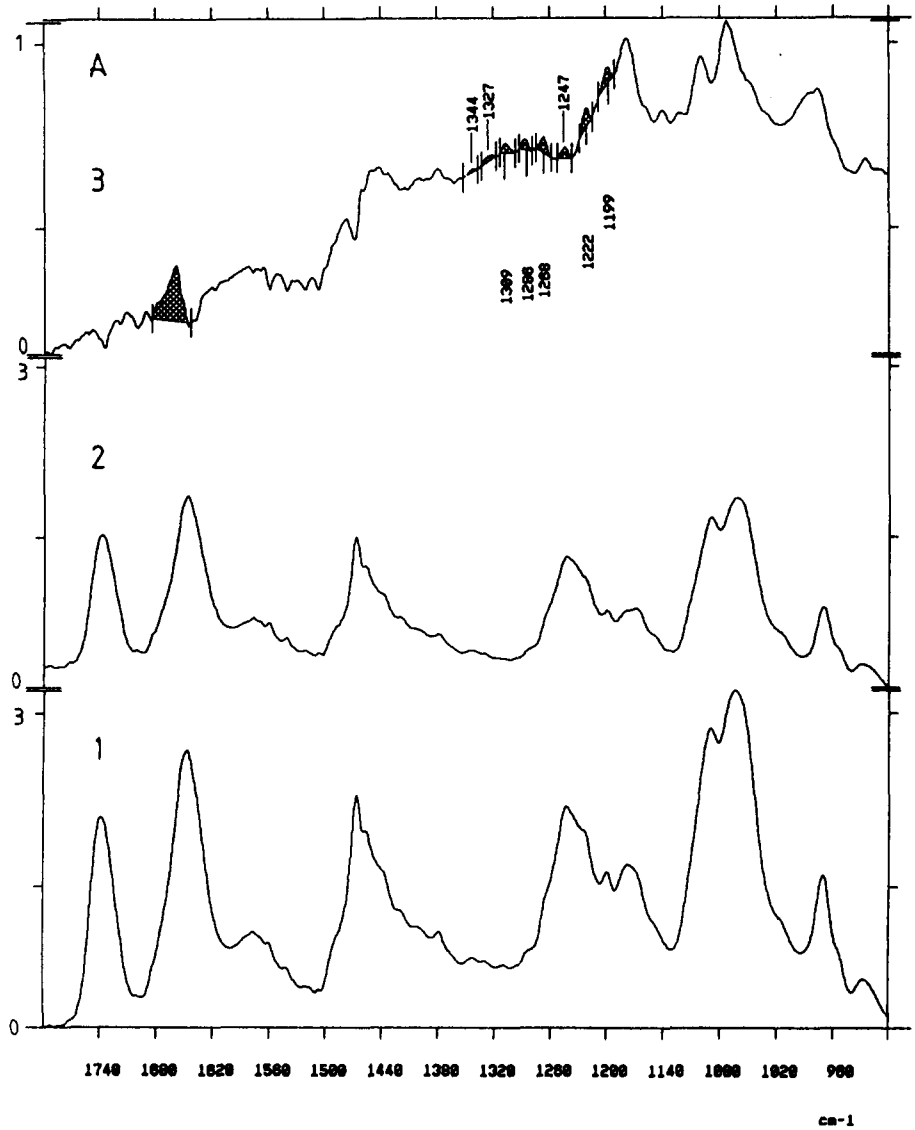

Fig. 3. Infrared spectra recorded with 90°-polarized light (trace 1) and 0°-polarized light (trace 2). The dichroic spectrum (trace 3) is obtained by subtraction of the spectrum recorded with a 0° polarization (trace 2) from the spectrum recorded with a polarization of 90°(trace 1), expanded three-fold in the ordinate direction. A positive deviation on the dichroic spectrum is representative of a dipole oriented preferentially close to a normal to the plane of the Ge plate, while a larger absorbance at 0° (negative deviation) means a dipole oriented close to the Ge crystal plane. All the samples were deuterated as described in Materials and Methods. (A) Apo A-IV/DPPC complexes (30 μg apo A-IV): the amide-I′ polarisation and the bands that belong to the $\gamma_w(CH_2)$ progression have been shaded on the dichroic spectrum (trace 3). (B) Pure DPPC (100 μg): the bands that belong to the $\gamma_w(CH_2)$ progression have been shaded on the dichroic spectrum (trace 3).

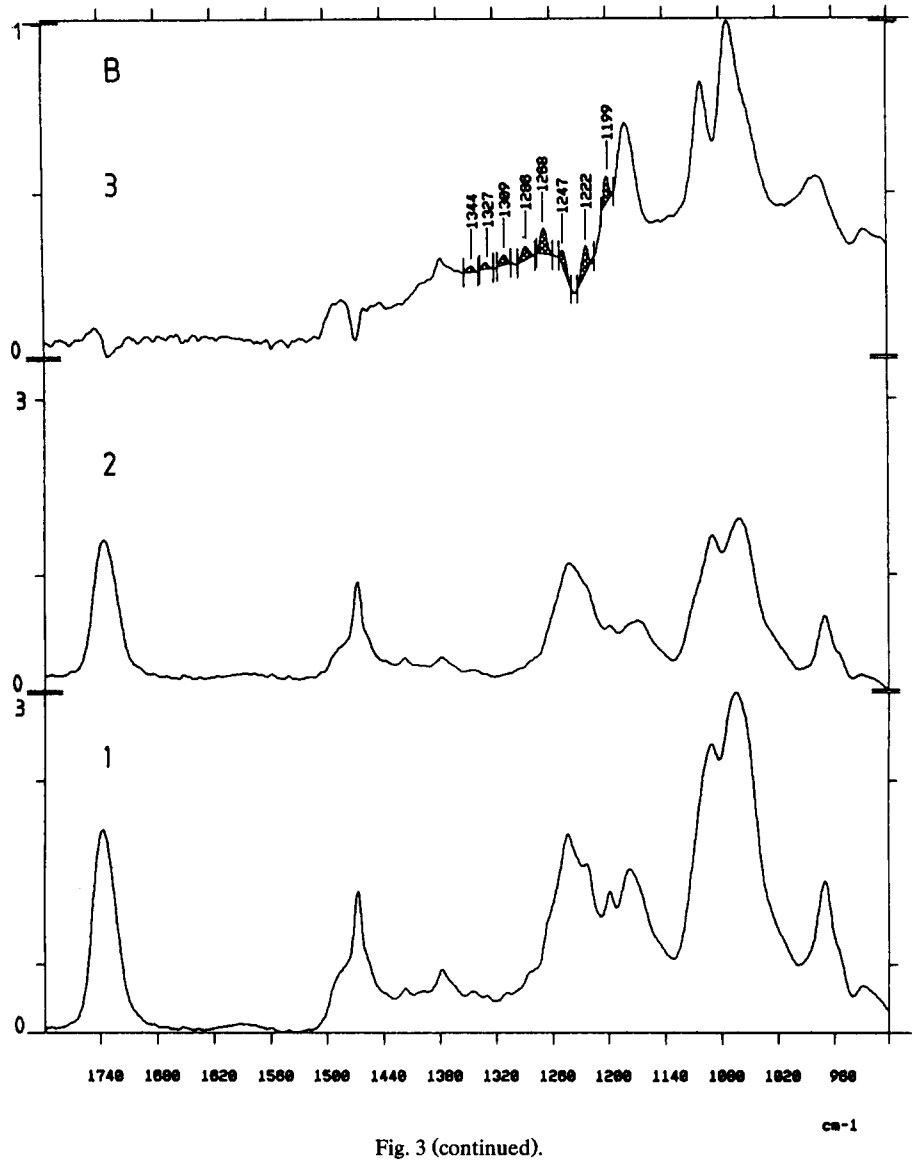

Fig. 3 (continued).

near 1180 cm^{-1} (Fig. 4A). On the other hand, the segment in the β-position is gauche, and the ν(C–O) vibration occurs near 1165 cm^{-1} (Fig. 4A). The ν(C–O) was deconvolved for both complexes by mean of Fourier self-deconvolution and curve fitting which allow a good resolution of both components (Fig. 4). The presence of the protein induces very little change at the level of the conformation, as well as of the orientation. Fig. 4A shows the 1200–1140 cm^{-1} deconvolved region for pure DPPC (Fig. 4A, curve 1) and apo A-IV/DPPC (Fig. 4A, curve 2). Apo A-IV does not modify the proportion of ester bonds in the planar conformation (maximum at 1180 cm^{-1}) and in the *gauche* conformation (maximum at 1167 cm^{-1}).

In the 90° and 0° polarized spectra (Fig. 4B,C), the 1182 cm^{-1} component is more intense at 90° than at 0° (C–O bond perpendicular to the bilayer plane) and the 1167 cm^{-1} peak has a larger absorbance at 0° (C–O bond parallel to the lipid bilayer plane). Since apo A-IV does not modify this pattern, it can be concluded that no major re-orientation occurs following the complex formation between apo A-IV and DPPC or DMPC.

TABLE III

Determination of the dichroic ratios of the phospholipids and apo A-IV α-helices

	Phospholipids		α-helix	
	R_{ATR} **	angle * (°)	R_{ATR} **	angle * (°)
Apo A-IV IV/DMPC	7.1	14	1.65	25
Apo A-IV/DPPC	4.5	18	1.60	27
Pure DMPC	6.3	15	–	–
Pure DPPC	3.2	23	–	–

* Angle between the CH_2 dipole moment or helix axis and a normal to the germanium plate.

** Calculated as mentioned in Materials and Methods.

Concerning the phosphocholine region (1238 cm^{-1}, 1091 and 1071 cm^{-1}), the minor changes observed on the spectra of reconstituted particles cannot be related to a significant change in the phosphocholine organization or orientation.

Discussion

As discoidal particles composed of lipids and apo A-IV have been identified in the peripheral lymph of cholesterol fed animals and in humans, we prepared and isolated particles containing apo A-IV and DMPC or DPPC. These complexes were formed by incubation of the DMPC phospholipid vesicles with apo A-IV or by the cholate dialysis procedure, for the apo A-IV-DPPC complexes as described for apo A-I [36].

The resulting complexes were isolated by gel filtration and characterized in terms of their size, composition, conformation and orientation of apo A-IV and lipid conformation. The apo A-IV/DMPC reconstitution gives rise to large discs (diameter approx. 140 Å) as observed by GGE and electron microscopy; the apo A-IV/DPPC complex has a 20 Å smaller diameter (approx. 120 Å). No attempt was made here to separate the subclasses of apo A-IV discoidal complexes, since the determined Stokes diameters vary between

TABLE IV

	nb helices/apo A-IV calculated from IR data	Diameter (Å) from GGE exp.	P (Å) *	nb of helices per apo A-IV **
DPPC complex	9–10	120	336	9
DMPC complex	11–12	140	440	12

* $P = 2\pi(D_{exp} - D_2)/2$, where D_{exp} is deduced from GGE experiments and represents the mean external diameter (D_{out} in Scheme I below) and D_2 represents the mean small diameter of the apo A-IV helices (Scheme I).
$(D_{exp} - D_2)/2$ represents the diameter of the circle on which the centers of the helices are aligned

** Calculated as follows: $(P/18)/2$ where 18 represents the mean distance in Å between the centers of two adjacent helices (d, see Scheme I). The number of helices are divided by 2 to determine the number of helices per apo A-IV molecule.

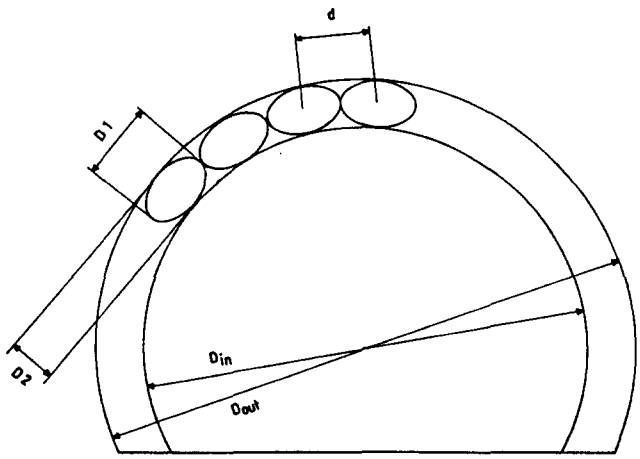

Scheme I

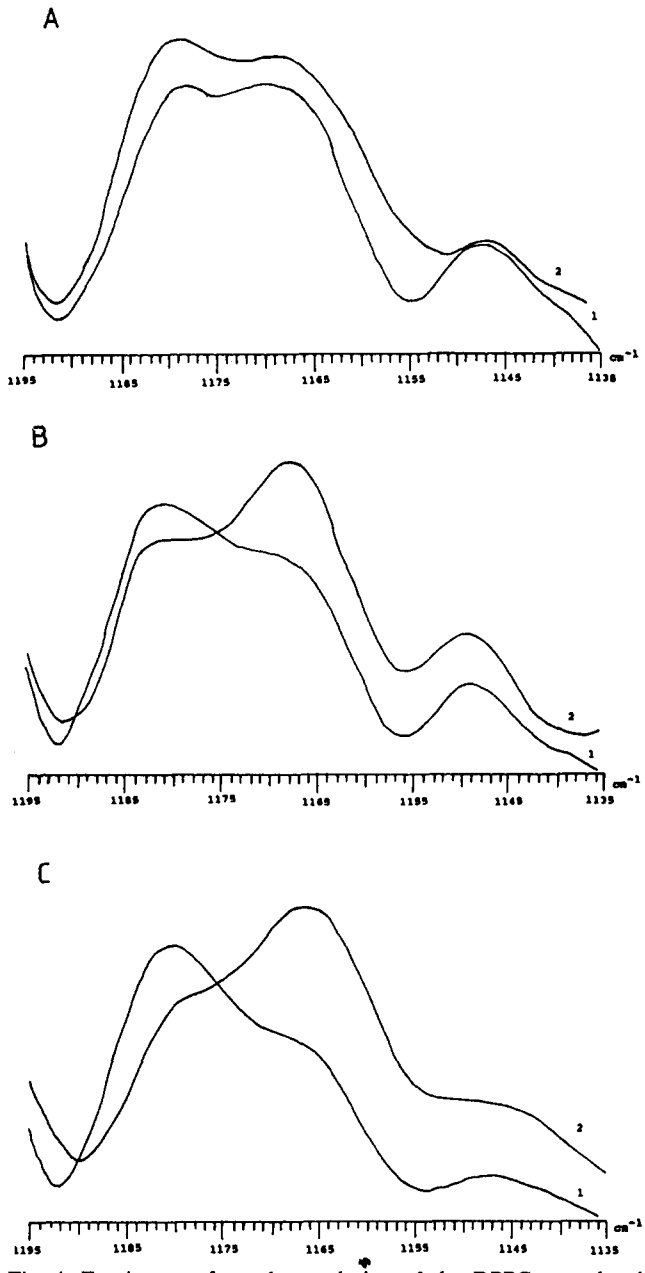

Fig. 4. Fourier transform deconvolution of the DPPC ester band (1135–1195 cm^{-1}) into its α (1180 cm^{-1}) and β (1167 cm^{-1}) components. (Panel A) Deconvolution of the non-polarized spectra of: 1, apo A-IV/DPPC complexes; 2, pure DPPC. (Panel B) Polarized spectra of the α and β components of the apo A-IV/DPPC complex. 1, Spectrum recorded with 90°-polarized light; 2, spectrum recorded with 0°-polarized light. (Panel C) Polarized spectra of the α and β components of pure DPPC. 1, Spectrum recorded with 90°-polarized light; 2, spectrum recorded with 0°-polarized light.

134 and 150 Å for the DMPC-apo A-IV complexes and between 112 and 124 Å for the DPPC complexes. For a reaction mixture containing dipalmitoylphosphatidylcholine, cholesterol and apo A-I in a 150:7.5:1 molar ratio, the particles were separated into three classes of lipid discs with diameter of 97, 136 and 186 Å and containing 2, 3 and 4 molecules of apo A-I per disc [42]. Despite this large size variety, the secondary structure of apo A-I was shown to be comparable for the three complexes [24,42].

Binding to PC increases the apo A-IV helicity, from 35% to 45% in the DPPC reconstitution and from 35% to 55% in the DMPC/apo A-IV complexes. This different behavior between the DPPC and DMPC particles has not been observed with apo A-I [24,25], whose helicity increases from 30% to 45–50% when bound to a DMPC or DPPC bilayer [23–25]. Like apo A-I [24,25,43] or E (unpublished results), the helical segments of apo A-IV are oriented mainly parallel to the PC acyl chains in both reconstitutions, confirming the general mode of organization of the apolipoproteins around the phospholipid bilayer [24,25,44].

The increase in size and helicity in apo A-IV/DMPC particles as compared to apo A-IV/DPPC could be explained in terms of the number of apo A-IV helical segments located around the edge of the disc. Indeed, as apo A-IV contains 376 residues, the percentage of α-helix in the DPPC and DMPC complexes, deduced from the IR data, corresponds to 9–10 and 11–12 helical segments per apo A-IV (Table IV), respectively, if we consider that an α-helix of the apolipoprotein class is made of 18 amino acids [43,44]. A theoretical number of helices around the edge of the DMPC and DPPC/apo A-IV discs can be calculated from the experimental diameters determined by GGE and from the mean distance between the centers of two adjacent helices (18 Å) and the mean small diameter (13 Å) of the apo A-IV helices as described [43,44] (Table IV). Indeed, the cross-section of the helices of apo A-IV is ellipsoidal because of the distribution and the volume occupied by the amino-acid lateral chains (lysyl and arginyl residues) [43,44]. From these data, the mean perimeter (P) of each complex is calculated, considering two molecules of apo A-IV associated to the DMPC [43] and DPPC complex (data not shown), as determined by cross-linking experiments (Table IV). Table IV illustrates the agreement between the number of helices per apo A-IV deduced from the IR data and the number estimated from the diameters determined experimentally. A difference of 2–3 helical segments per apo A-IV is effectively observed between the DMPC and the DPPC complexes. This result could be related to the behavior of apo A-IV bound to a phospholipid monolayer. Weinberg et al. have suggested that at a low surface pressure, all the amphipathic helices of apo A-IV are able to bind the lipids, while at higher surface pressures, some of these helical segments do no longer bind to the monolayer [12].

Predictive analysis of the apo A-IV sequence may suggest that the domains characterized by a weak affinity for the lipids are located on the N-terminus of apo A-IV. Here, the hydrophobic cluster analysis (HCA) method, developed by Gaboriaud et al. [45] has been applied to apo A-IV (Fig. 5). Briefly, this method is based on an α-helical two-dimensional representation of protein sequences, where the size, shape and composition of clusters of hydrophobic residues are analyzed and compared. In this method, long, horizontal hydrophobic clusters (pho residues are circled and hatched) that are well separated by clear hydrophilic areas denote amphipathic α-helices and vertical or 'mosaic' hydrophobic clusters are indicative of β-strands or β-sheets [46]. The apo A-IV sequence, analyzed by the HCA technique (Fig. 5), revealed, for the N-terminal domain, a heterogeneous (mosaic) distribution of the hydrophobic residues which is probably related to a β-sheet or a β-strand structure. The 40–70 N-terminal region may be related to an amphipathic helical region but compared to the 70–350 C-terminal part, its amphipathicity is less pronounced: the 70–350 region indeed shows more horizontal hydrophobic clusters than the 40–70 N-terminal domain whose hydrophobic clusters are more oblique. Two other domains can also be distinguished in the apo A-IV se-

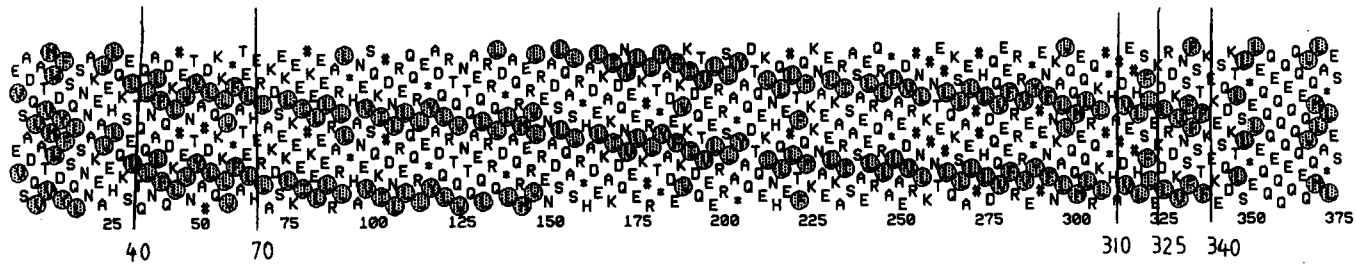

Fig. 5. 2-D α-helical patterns of HCA analysis for apo A-IV sequence. The sequence is written on a classical α-helix (3.6 amino acid per turn) smoothed on a cylinder. To make the 3-D representation easier to handle, the cylinder is then cut parallel to its axis and unrolled. As some adjacent amino acids are separated by the unfolding of the cylinder, the representation is duplicated to restore the full connection of each amino acid. The hydrophobic residues (VLIMYW) are circled and hatched; Pro is represented by * and Gly by #. The vertical lines separate the

quence. First, from about residue 310 to residue 325, the hydrophobic cluster is more vertical. This region corresponds in fact to a loop between two amphipathic α-helices (291–308 and 324–341) [43,44]. Second, the C-terminus [340–376] contains no horizontal hydrophobic clusters and characterizes a β-sheet or a β-strand.

Since amphipathicity has been shown to strongly enhance the lipid–peptide association, the decreased amphipathicity associated to residues 43–60 and 64–81 which correspond to the first and second amphipathic helices predicted to be associated to the discoidal lipid structure [43,44,47], may explain their lower affinity for the lipids.

Concerning the phospholipid conformation and orientation after complex formation:

(1) a significant decrease (25%) in the proportion of the all-*trans* conformation of the DPPC and DMPC acyl chains is observed when apo A-IV is bound to these phospholipids. This decrease could be explained either by a conformational modification of 25% of the hydrocarbon chains, like the appearance of a kink in the CH_2 progression or by a modification of the phospholipid ester group of all the PC. Deconvolution of the 1190–1150 cm^{-1} domain of the IR spectra revealed no significant change in the proportion of the planar and gauche components of the ester group as well as no major re-orientation of both components. As the ester bonds were not responsible for the decrease in the proportion of the all-*trans* acyl chains, we assumed that the conformation of the phospholipid hydrocarbon chains in close contact with apo A-IV were modified, as 20–25% of the total calculated amount of lipids in the discoidal particle are adjacent to the apo A-IV amphipathic helices.

It is worth noting that we observed the same decrease in the proportion of the all-*trans* conformation of the acyl chains when apo A-I was reconstituted with DPPC, but, in this case, the decrease was assigned to a reorientation of the ester group [24].

(2) We observed no significant increase of the dichroic ratio associated to the DMPC or DPPC acyl chains when these lipids are bound to apo A-IV. The ordering of the lipid molecules or the straightening of the hydrocarbon chains associated to the apo A-I/DPPC smallest particles [24] can not be demonstrated here. However, it should be mentioned that for apo A-I, these effects were no more significant for DPPC/apo A-I complexes with a diameter similar to that of the apo A-IV-lipid complexes studied here [24]. From this point of view, apo A-I and apo A-IV show similar behavior.

As a general conclusion, apo A-IV forms stable discoidal complexes with either DMPC or DPPC. The different sizes of the apo A-IV-phospholipids complexes can be explained in terms of a variable number of amphipathic helices per apo A-IV bound to the edge of the lipid disc. Apo A-IV does not perturb the phospholipid conformation and orientation in a significant way, even if the apo A-IV-phospholipid complexes, used in this work, are more heterogeneous in size and composition as compared to the apo A-I/DPPC particles.

Acknowledgements

One of us (L.L.) wants to thank IRSIA (Institut pour l'encouragement de la Recherche Scientifique dans l'Industrie et l'Agriculture) for financial support. R. Brasseur is a Senior Research Assistant for the National Fund for Scientific Research.

References

1 Swaney, J.B., Reese, H. and Eder, H.A. (1974) Biochem. Biophys. Res. Commun. 59, 513–519.
2 Weisgraber, W.H., Bersot, T.P. and Mahley, R.W. (1978) Biochem. Biophys. Res. Commun. 85, 287–292.
3 Beisiegel, U. and Utermann, G., (1979) Eur. J. Biochem. 93, 601–608.
4 Fidge, N.H. and Nestel, P. (1981) Circulation 64 (Suppl. IV) 159A.
5 Weinberg, R.B. and Spector, M.S. (1985) J. Lipid Res. 26, 26–37.
6 Bisgaier, C.L., Sachdev, O.P., Megna, L. and Glickman, R.M. (1985) J. Lipid Res. 26, 11–25.
7 Ghiselli, G., Krishnan, S., Biegel, Y. and Gotto, A.M. (1986) J. Lipid Res. 27, 813–827.
8 Delamatre, J.G., Hoffmeier, C.A., Lacko, A.G. and Roheim, P.S. (1983) J. Lipid Res. 24, 1578–1585.
9 Weinberg, R.B. and Spector, M.S. (1986) Biochem. Biophys. Res. Commun. 135, 756–763.
10 Bisgaier, C.L., Sachdev, O.P., Lee, E.S., Williams, K.J., Blum, C.B. and Glickman, R.M. (1987) J. Lipid Res. 28, 693–703.
11 Bisgaier, C.L., Siebenkas, M.V., Hesler, C.B., Swenson, T.L., Blum, C.B., Marcel, Y.L., Milne, R.W., Glickman, R.M. and Tall, A.R. (1989) J. Lipid Res. 30, 1025–1031.
12 Weinberg, R.B., Ibdah, J.A., Phillips, M.C., (1992) J. Biol. Chem. 267, 8977–8983.
13 Stein, O., Stein, Y., Lefevre, M. and Roheim, P.S. (1986) Biochim. Biophys. Acta 878, 7–13.
14 Steinmetz, A., Barbaras, R., Ghalim, N., Clavey, V., Fruchart, J.C. and Ailhaud, G. (1990) J. Biol. Chem. 265, 7859–7863.
15 Ghiselli, G., Crump, W.L. and Gotto, A.M. (1986) Biochem. Biophys. Res. Commun. 139, 122–128.
16 Dvorin, E., Gorder, N.L., Benson, D.M. and Gotto, A.M. (1986) J. Biol. Chem. 261, 15714–15718.
17 Savion, N., Gamliel, A., Tauber, J.P. and Gospodarowicz, D. (1987) Eur. J. Biochem. 164, 435–443.
18 Savion, N. and Gamliel, A. (1988) Arteriosclerosis 8, 178–186.
19 Steinmetz, A. and Utermann, G. (1985) J. Biol. Chem. 260, 2258–2264.
20 Chen, C.H. and Albers, J.J. (1985) Biochim. Biophys. Acta 836, 279–295.
21 Sloop, C.H., Dory, L. and Roheim, P.S. (1987) J. Lipid Res. 28, 225–237.
22 Puchois, P., Steinmetz, A., Ghalim, N., Barbaras, R., Barkia, A., Ailhaud, G. and Fruchart, J.C. (1988) Circulation 78 (Suppl. II), 168.
23 Jonas, A., (1984) Exp. Lung Res. 6, 255–270.
24 Wald, J.H., Goormaghtigh, E., De Meutter, J., Ruysschaert, J.M. and Jonas, A. (1990) J. Biol. Chem. 265, 20044–20050.

25 Brasseur, R., De Meutter, J., Vanloo, B., Goormaghtigh, E., Ruysschaert, J.M. and Rosseneu, M., (1990) Biochim. Biophys. Acta 1043, 245–252.
26 Krebs, K.E., Ibdah, J.A. and Phillips, M.C. (1988) Biochim. Biophys. Acta 959, 229–237.
27 Ibdah, J.A. and Phillips, M.C. (1988) Biochemistry 27, 7155–7162.
28 Ibdah, J.A., Krebs, K.E. and Phillips, M.C. (1989) Biochim. Biophys. Acta 1004, 300–308.
29 Weinberg, R.B. and Jordan, M.K., (1990) J. Biol. Chem. 265, 8081–8086.
30 Cabiaux, V., Brasseur, R., Wattiez, R., Falmagne, P., Ruysschaert, J.M. and Goormaghtigh, E. (1989) J. Biol. Chem. 264, 4928–4939.
31 Goormaghtigh, E., Martin, I., Vandenbranden, M., Brasseur, R. and Ruysschaert, J.M. (1989) Biochem. Biophys. Res. Commun. 198, 610–616.
32 Goormaghtigh, E., De Meuter, J., Cabiaux, V., Szoka, F. and Ruysschaert, J.M., (1991) Eur. J. Biochem. 195, 421–429.
33 Goormaghtigh, E., Vigneron, L., Kniebiehler, M., Ladzunski, C. and Ruysschaert, J.M. (1991) Eur. J. Biochem. 202, 1299–1305.
34 Demel, D.A., Goormaghtigh, E. and De Kruijff, B. (1990) Biochim. Biophys. Acta 1027, 155–162.
35 Yang, C.Y., Gu, Z.W., Chang, I., Xing, W., Rosseneu, M., Yang, H.X., Lee, B.R., Gotto, A.M. and Chan, L. (1989) Biochim. Biophys. Acta 1002, 231–237.
36 Matz, C.E. and Jonas, A. (1982) J. Biol. Chem. 257, 4535–4540.
37 Vanloo, B., Morrison, J., Fidge, N., Lins, L., Lorent, G., Brasseur, R., Ruysschaert, J.M. Baert, G. and Rosseneu, M. (1991) J. Lipid Res. 32, 1253–1264.
38 Goormaghtigh, E., De Meutter, J., Vanloo, B., Brasseur, R., Rosseneu, M. and Ruysschaert, J.M. (1989) Biochim. Biophys. Acta 1006, 147–150.
39 Cortijo, M., Alonso, A., Gomez-Fernandez, J.C. and Chapman, D. (1982) J. Mol. Biol. 157, 579–618.
40 Hayat, M.A. and Miller, S.E. (1990) in Negative staining, McGraw-Hill, New York.
41 Jonas, A., Kezdy, K.E. and Wald, J.H. (1989) J. Biol. Chem. 264, 4818–4824.
42 Wald, H.J., Krul, E.S. and Jonas, A. (1990) J. Biol. Chem. 265, 20037–20043.
43 Lins, L., Brasseur, R., Vanloo, B., Ruysschaert, J.M. and M. Rosseneu, (1992) in Structure and function of apolipoproteins (Rosseneu, M., ed.), pp. 251–268, CRC Press, Boca Raton.
44 Brasseur, R., Lins, L., Vanloo, B., Ruysschaert, J.M. and Rosseneu, M. (1992) Proteins 13, 246–257.
45 Gaboriaud, C., Bissery, V., Benchetrit, T. and Mornon, J.P. (1987) FEBS Lett. 224, 149–155.
46 Lemesle-Varloot, L., Henrissat, B., Gaboriaud, C., Bissery, V., Morgat, A. and Mornon, J.P. (1990) Biochimie 72, 555–574.
47 Li, W.H., Tanimura, M., Luo, C.C., Datta, S. and Chan, L. (1988) J. Lipid Res. 29, 245–271.